CI

e-med
www.e-med.org.uk

REVIEW ARTICLE

Magnetic resonance perfusion imaging in neuro-oncology

Alan Jackson, James O'Connor, Gerard Thompson and Samantha Mills

*Division of Imaging Science, University of Manchester, Wolfson Molecular Imaging Centre,
27 Palatine Road, Manchester, M20 3LJ, UK*

*Corresponding address: Professor Alan Jackson, Division of Imaging Science, University of Manchester,
Wolfson Molecular Imaging Centre, 27 Palatine Road, Manchester, M20 3LJ, UK.
Email:* `alan.jackson@manchester.ac.uk`

Abstract

Recent advances in magnetic resonance imaging (MRI) have seen the development of techniques that allow quantitative imaging of a number of anatomical and physiological descriptors. These techniques have been increasingly applied to cancer imaging where they can provide some insight into tumour microvascular structure and physiology. This review details technical approaches and application of quantitative MRI, focusing particularly on perfusion imaging and its role in neuro-oncology.

Keywords: *Magnetic resonance imaging (MRI); functional imaging; dynamic imaging; perfusion; permeability; glioma; meningioma; cerebral tumour.*

Introduction

The past 20 years have seen substantial and ongoing improvements in the technical capability of computed tomography (CT) and magnetic resonance imaging (MRI). Modern systems can reliably produce clinical images with higher spatial resolution and greater volume coverage, over a shorter time frame than was previously possible[1]. Concurrently, there has been an increasing demand for images which represent and quantify specific aspects of tissue structure and function, such as blood flow or blood volume.

Quantitative images of anatomical and physiological features have additional clinical utility to conventional imaging. They are, in theory, independent of the imaging modality or scanning system used. Resultant images are referred to as *parametric imaging* since the individual pixel values are calculated parameters derived from primary imaging data. These parameters are, in turn, *imaging biomarkers* as they represent 'a characteristic that is objectively measured and evaluated as an indicator of normal biological processes or pathogenic processes or pharmacological responses to therapeutic intervention'[2]. Imaging biomarkers have become important tools when investigating the microvasculature characteristics of normal and pathological tissues.

One common application of quantitative biomarker imaging is 'perfusion imaging' – a commonly used term that is in fact a misnomer. Perfusion describes the process by which blood flow through a tissue provides nutrition and removes metabolic byproducts. Imaging techniques traditionally used to quantify perfusion include $H_2^{15}O$ positron emission tomography (PET) and xenon-enhanced CT. In both techniques the tracer is delivered to the tissue and leaves the vasculature producing changes in signal which directly reflect flow to the tissue exchange capillaries, producing a true measurement of perfusion. In some circumstances large vessels may pass through a voxel which have measurable flow but do not contribute to the local tissue perfusion.

Perfusion and blood flow are not the only imaging biomarkers of microvascular structure and function widely used (Fig. 1). In cancer imaging, measurements of proportional blood volume, endothelial capillary permeability or vessel size are of equal or greater importance. One of the major drives to develop these imaging biomarkers has been the development of novel therapeutic agents designed to treat cancer by inhibiting angiogenesis or disrupting immature neovasculature[3–6]. In pathological tissues the angiogenic process is often abnormal, leading to the development of distorted vascular beds characterized
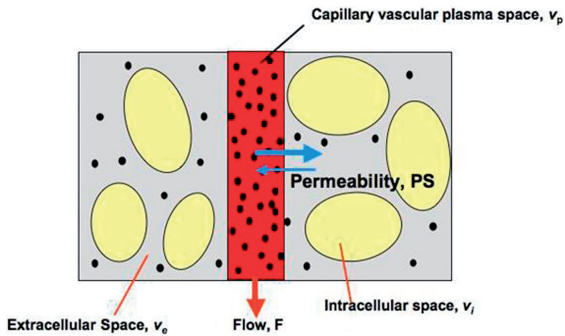
Figure 1 **Diagram representing compartmental modelling of the tumour microvasculature. Blood flows through the tumour enabling contrast media molecules (represented by the black dots) to distribute into two potential compartments: the blood plasma volume, v_p, and the extravascular extracellular space, v_e. MRI contrast agents that are used clinically do not pass into the intracellular space, v_i. Contrast leakage is governed by the concentration difference between the plasma and the extracellular extravascular space and by the permeability and the surface area of the capillary endothelia expressed as *PS*. Adapted from O'Connor *et al.*[6] by permission from Macmillan Publishers Ltd, British Journal of Cancer, © 2007.**

by an excessive proportion of blood vessels and blood vessels with abnormal morphology and flow characteristics[7]. Central areas of a rapidly growing tumour commonly exhibit inadequate blood flow due to reduced local perfusion pressure resulting from a combination of inadequate vascularization and increased interstitial tumour pressure. Finally, the angiogenic neovasculature will exhibit increased endothelial permeability to medium and large sized molecules[8,9]. It is important to realize that this increase in vascular permeability is most commonly a direct effect of cytokine stimulation and can be rapidly reversed by inhibition of the active cytokine[5]. In contrast, vascular density, vascular tortuosity and other abnormalities of vascular structure represent the cumulative effects of the angiogenic process that has occurred to date. Because of this the biological information contained in these two groups of measurements offers distinct and separate insight into the status of the angiogenic process.

Neuro-oncology has been one of the main areas in which imaging biomarkers have been widely applied. This article reviews the technical approaches to 'perfusion MRI' and describe the applications of these techniques to date.

Techniques of perfusion imaging

At the present time there are three widely used generic approaches to the measurement of regional cerebral blood flow in humans:

1. Measurement based on the kinetics of a freely diffusible tracer, most commonly either xenon imaged with dynamic CT or $H_2^{15}O$ imaged with PET.
2. Measurements based on the inflow of magnetically labelled water into the tissue using arterial spin labelling (ASL) with MRI.
3. Measurements based on the kinetics of a short-lived bolus of an intravascular contrast agent, most commonly iodine-containing contrast agents imaged with dynamic contrast-enhanced CT (DCE-CT) or gadolinium-containing contrast agents imaged with dynamic contrast-enhanced MRI (DCE-MRI).

The first group of techniques are considered 'gold standard' since the markers have an extremely high transfer coefficient and their concentration in brain tissue can be considered to be dependent entirely upon vascular concentration and flow. Both $H_2^{15}O$-PET and xenon enhanced CT use is limited by cost, availability and methodological problems. In contrast, the ability to characterize the microvasculature using biomarkers produced by CT and MRI, which are widely available, using clinical contrast agents is highly attractive and has been the main thrust of research in the area.

Arterial spin labelling

The overall goal of all existing ASL techniques is to produce a flow-sensitized 'labelled' image and a 'control' image in which the static tissue signals are identical, but where the magnetization of the in-flowing blood differs. The subtraction control label yields a signal difference that directly reflects local perfusion because the signal from stationary tissue is completely eliminated. The label is usually performed by inverting or saturating the water molecules of the blood supplying the imaged region. By adding a delay between labelling and image acquisition, called inversion delay, the labelled blood spins are allowed to reach the capillaries where they exchange with tissue water and thereby give rise to the perfusion signal. The signal difference, which is only around 0.5–2% of the full signal, depends on many parameters such as the flow, T1 of blood and tissue, and the time taken for blood to travel from the labelling to the imaging region. Multiple pulse repetitions are needed to ensure a sufficient signal-to noise ratio, and a model of the perfusion signal is usually used in order to quantify the perfusion.

There are two main classes of ASL techniques: continuous ASL (CASL) and pulsed ASL (PASL)[10–12]. In CASL, the supplying blood is continuously labelled below the imaging slab, until the tissue magnetization reaches a steady state. The PASL approach labels a thick slab of arterial blood at a single instance in time, and the imaging is performed after a sufficient time to allow the spatially labelled blood to reach the tissue and exchange at the region of interest. Both methods need a control experiment in order to visualize and quantify the perfusion. Magnetic labelling of inflowing blood will

be subject to the same energy loss mechanisms observed for any MRI experiments. Thus T1 labelling will last only 1–2 s depending on the sensitivity of the system. Add to this a problem that maximum signal changes are only small (1–2%) and therefore the technique is extremely demanding. The actual interpretation of flow measurement depends on the methodology applied for the labelling process and the subsequent analysis[13]. Recent developments have led to relatively robust and sensitive techniques which are able to identify even small blood flow related to cerebral functional activation.

Dynamic contrast-enhanced (DCE) imaging

These techniques use rapid measurements of changes in CT attenuation or MR signal during the injection of a bolus of conventional clinical contrast agent[14,15]. The signal changes resulting from the first passage of the contrast agent bolus can be used to calculate estimates of cerebral blood volume (CBV), mean transit time (MTT) and cerebral blood flow (CBF)[16]. DCE-MRI is simple to perform in a clinical environment and is now the MR perfusion technique most commonly used in clinical studies[17,18]. The conventional approach to modelling cerebral blood flow from DCE data relies upon three key assumptions: (1) that contrast concentration is predictably related to signal change; (2) that the integrated contrast concentration is predictably related to the blood volume in the measurement space; and (3) that the shape of the contrast concentration distribution curve is governed by the mean transit time of contrast through the measurement space.

Dynamic susceptibility contrast-enhanced imaging (DSCE-MRI)

T2 and T2* dynamic imaging acquisitions have been widely used in the brain[17]. The susceptibility effect of contrast media extends to tissues surrounding blood vessels so that the signal change on T2*-weighted images is effectively amplified in the presence of sparse capillary beds where the blood volume within the tissue is low[19–21]. Signal changes observed during the passage of a contrast bolus through the vessels can be transformed to contrast concentration maps from which quantitative images of physiological parameters may be derived.

Several analysis techniques have been described. A common feature of many is the use of a gamma variate fitting procedure to define the shape and position of the first pass bolus. The need for this step arises from the signal changes occurring after the passage of the contrast bolus as contrast recirculates into the cerebral circulation from the periphery. As a result of this recirculation, the contrast concentration fails to return to pre-enhancement levels. Parametric images of regional blood volume

(rCBV) can be derived from the area under the contrast concentration–time course curve and indicators of bolus arrival time may also be accurately calculated. Measurements of absolute blood flow are more complicated and subject to errors due to effects such as bolus dispersion and arrival time delays[22]. Where extravascular leakage of contrast occurs the T2* effect of intra-vascular contrast will cause signal loss, whereas the predominant T1 effect of extravascular contrast will cause an opposing signal increase. This effect, known as 'T1 shine through', can be reduced[7] to allow accurate measurement of blood volume.

Quantification of contrast leakage to produce measures of contrast transfer coefficient (K^{trans}) is more difficult[23]. T2 and T2* techniques also suffer from serious susceptibility artefacts in the presence of interfaces between air/fat and soft tissue so that their use has been limited to studies of normal brain and brain tumours. One advantage of T2-based techniques is the ability to estimate the average vessel size within the tissue using measurements from both T2- and T2*-weighted images. This has one specific application in testing the hypothesis of vascular normalization following anti-angiogenic treatment[24–26]. Another interesting application is quantifying any abnormal elevation of the contrast concentration in the period immediately after the passage of the contrast bolus, referred to as 'relative recirculation' (rR)[7]. In theory the rR will be increased by local vascular factors such as absolute flow rate, flow rate heterogeneity and therefore by decreases in local perfusion pressure.

Dynamic relaxivity contrast-enhanced MRI (DRCE-MRI)

Most DCE-MRI studies employ T1-weighted images which are free from susceptibility artefacts. The choice of imaging sequence is driven by a number of factors which vary from study to study[27]. The temporal resolution of the imaging sequence is dictated by the analysis technique chosen. Where the analysis requires accurate measurement of the change in contrast concentration in plasma (commonly called the arterial input function, AIF), then a high temporal resolution, usually of 5 s or less, will be essential[28].This limits the spatial resolution of the imaging sequence and the amount of tissue that can be imaged. AIF measurement is further complicated by flow artefacts, seen on many imaging sequences[4,29,30].

In order to provide adequate data for pharmacokinetic analysis (and thus modelled parameters, see below) data collection will typically continue for in excess of 5 min. Flow artefacts are usually negligible in all slices except for those at the edges of the volume, allowing accurate measurement of AIF. In the brain there is a particular problem with the larger arteries sited at the base of the brain and therefore inevitably at the margin of the imaging block. This can necessitate angled acquisitions
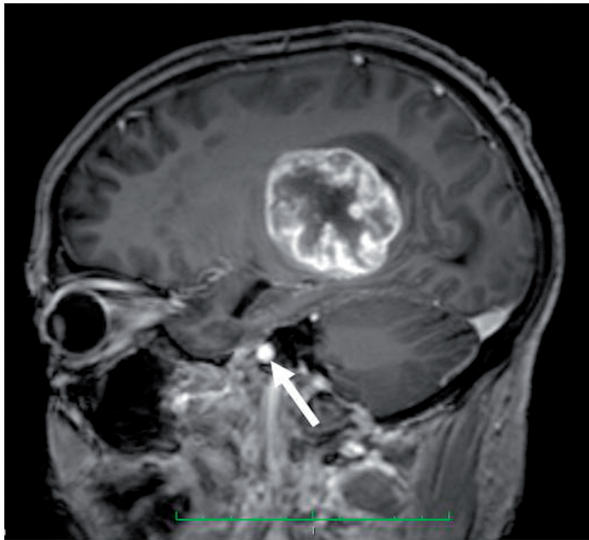
Figure 2 **Sagittal oblique acquisition to incorporate the internal carotid artery (white arrow) and tumour.**

to include both the tumour and a major artery within the imaging field (Fig. 2).

Pharmacokinetic analysis of contrast distribution requires transformation of measurements of signal change over time to measurements of contrast concentration[31]. For T1-weighted data the relationship between signal change and contrast concentration is non-linear so it is necessary to measure the baseline T1 of each voxel prior to contrast injection. This can be time consuming and complex. Most centres have developed quantification methods using multiple T1-weighted images acquired with varying flip angles to allow T1 calculations[4].

Analysis of DCE-MRI data

A number of early studies attempted to quantify changes in contrast enhancement using measurements of signal change which avoids the complexity of calculating contrast concentrations. Such metrics characterize the shape of the signal time course curve or compare the increase in signal intensity achieved in a given period of time[32,33]. These simple metrics are unpredictably affected by variations in scanning protocol, which adversely affects reproducibility, and does not distinguish signal changes due to variations in blood flow, blood volume and contrast leakage[34]. Despite this, simple measurements based on signal change alone can be diagnostically useful and have found application in a number of clinical situations[9,35–38].

Most longitudinal studies employ more complex pharmacokinetic analysis techniques, which have several potential advantages[39–41]. Derived parameters are theoretically independent of the scanning acquisition protocol and should reflect only tissue characteristics, allowing their use in multi-centre studies[5,42]. In practice,

pharmacokinetic analysis is complex and the choice of model has major impact on the interpretation of the derived parameters. One of the simplest parameters is the integrated area under the contrast concentration curve (IAUC) which is easy to perform, appears reproducible but offers no biological specificity[31,43,44]. All other pharmacokinetic analyses use curve fitting techniques to characterize the tissue contrast concentration curve. This function is then used, together with an AIF, to derive the parameters which control the relationship between the AIF and tissue contrast content. The AIF may be estimated or measured in which case it is characterized by a separate curve fitting process[28].

The simplest pharmacokinetic models, such as that described by Tofts and Kermode[41] calculate the size of the extravascular extracellular space (v_e) and the bulk transfer coefficient (K^{trans}), a constant which describes the relationship between the AIF and the contrast concentration changes occurring in the tissue. Measurements of K^{trans} will reflect changes in blood flow, blood volume, endothelial permeability and endothelial surface area and these individual effects cannot be distinguished. This simple model also assumes that signal changes result entirely from extravascular contrast which gives rise to significant errors in voxels that contain large vascular spaces.

Many workers have attempted to refine the pharmacokinetic analysis to provide more accurate estimates of individual microvascular parameters, particularly the signal contribution produced by contrast medium within plasma (v_p), regional blood flow (F) and the product of capillary endothelial permeability and capillary surface area (PS), which is directly affected by VEGF expression[5]. The basic model is commonly modified to specifically estimate v_b[40,45] so that K^{trans} will reflect contributions of F and PS. More complex models allow direct estimation of v_p, v_e and F so that K^{trans} will represent PS[46]. These models appear desirable since they allow specific analysis of biological effects. However, the increase in the number of variables involved in the curve fitting process produces concomitant reductions in accuracy and reproducibility. For these reasons the choice of pharmacokinetic model depends on the degree of specificity required with regard to the mechanism of drug action, the acceptable level of reproducibility in the estimation of biomarkers and the quality of the MR data which can be acquired. In practice, most clinical studies and trials of angiogenesis inhibitors use the simple Tofts and Kermode model despite its shortcomings[6].

Specific imaging biomarkers

Measurements must be precise and reproducible in order to produce a reliable biomarker. Furthermore, measurement techniques employed to quantify a biomarker should be robust to error and there should be a clear

and specific relationship between the measurement and the biological process[2]. In practice, this is a major problem with imaging biomarkers – both values and definitions of individual biomarkers can vary depending on the technique used to acquire them. The published literature can be confusing particular for the reader who does not fully appreciate the technical complexities of the analysis techniques. This short section reviews some of the causes of confusion which arise around the following individual biomarkers.

Flow (F)

Flow may be calculated from ASL (Fig. 3), dynamic-MRI or CT, $H_2{}^{15}O$ PET or Xe-CT. The latter two techniques are designed to measure capillary perfusion (the distinction between perfusion and flow has been described above). Similarly, DSCE-MRI is purported to measure capillary perfusion due to the relative amplification of signal from areas with a low CBV which occurs due to the susceptibility effect. In practice, flow measurements are based on a number of assumptions concerning the speed of contrast delivery to the pathological tissue and the identification of an appropriate AIF. In normal tissue, some corrections can be made in the analysis to allow for these errors, but in tumour tissue, where the nature and timing of the AIF cannot be assessed, the use of this technique to derive flow measurements is inappropriate[22,47–49]. T1-weighted dynamic-MRI can be analysed using a complex pharmacokinetic model to produce estimates of flow but this demands both high temporal resolution and good signal to noise ratio in the data and therefore this technique has not been widely employed[50].

K^{trans}

Many publications refer to K^{trans} as a measurement of either permeability or blood flow. In fact, as described above, the contrast transfer coefficient depends on the model used to calculate it. Measurements from a single compartment model will be affected by blood volume (BV), F and PS. Measurements from the adiabatic tissue homogeneity model[50] will separately reflect F, BV and PS but are likely to be subject to significant errors. In models which separately represent BV, K^{trans} will be affected by both F and PS and in these cases it is not possible to establish whether changes in K^{trans} reflect changes in F or PS[51]. In the presence of high blood flow PS will have the dominant effect, whereas in areas where flow is low enough to limit contrast delivery in relation to the rate of contrast leakage, then K^{trans} will predominantly reflect flow[52]. It should be emphasized that this important point is widely ignored by many investigators, where reduction in K^{trans} following drug administration is claimed as direct evidence for reduction in permeability. In truth, reduction in K^{trans} is consistent with permeability changes but may simply represent reduced flow, change in surface are, or a combination of both.

CBV

Most techniques for the measurement of blood volume produce a relative value which has no units. In many publications, the term relative cerebral blood volume (rCBV) is used to show that values from a tumour have been normalized to an area of 'normal tissue', most commonly contralateral white matter. In fact,

Figure 3 **(A) Transverse contrast-enhanced T1-weighted MR image shows a rim-enhancing tumour, histologically glioblastoma multiforme. (B) Blood flow map obtained with arterial spin labelling reveals high heterogeneity in total blood flow, which is seen highest in the central portion; from Warmuth *et al*.[80] with permission from the Radiological Society of North America.**

absolute measurements of CBV can be obtained by normalizing the measured values to the venous blood to produce a measurement expressed as a proportion or percentage. Further confusion is engendered by the common use of the term regional cerebral blood volume, usually an absolute measurement, which is often also abbreviated as rCBV. The current evidence suggests that measurements of CBV from DSCE and DRCE-MRI are not interchangeable, although they may be comparable with some analysis models[52,53].

Imaging biomarkers in neuro-oncology

Despite a large number of studies describing quantitative imaging angiogenesis in brain tumours, none of these techniques has yet passed into routine clinical use. There is, however, considerable evidence that these quantitative techniques can provide valuable clinical information concerning tumour type, tumour grade and therapeutic response.

Differential diagnosis of cerebral tumours

Abscess vs. tumour

One area of clinical application is in the differentiation between abscess and primary tumour. Both lesions may appear as ring-enhancing lesions with peripheral oedema on conventional MRI and CT. Perfusion-weighted imaging (DSCE-MRI) demonstrates a clear separation between CBV values in abscesses (less than 1%) and high-grade gliomas (>3%)[54–56]. Diagnostic specificity is increased if perfusion data are combined with measurements of apparent diffusion coefficient (ADC), which is lower in abscess[54,57,58].

Distinguishing tumour type

Over 15 years ago, simple metrics based on estimations of the time taken to reach maximal enhancement or some proportion of maximal enhancement was shown to relate to tumour type[59,60]. Comparison of rCBV values between common extra-axial tumours and typical enhancing intra-axial tumours have shown the extra-axial masses to typically have higher values[61]. Meningiomas also had higher values of rCBV (as measured by both DSCE-MRI and DRCE-MRI) than those seen in neurinomas or schwannomas[4,8,61–63]. In addition, measurements of v_e were found to be higher in meningioma than in glioma and were consistently highest in acoustic neuroma[4]. These results agree with those of previous investigators[64] who demonstrated very large extracellular spaces in schwannomas using fluorescence electron microscopy. It has also been suggested that DSCE-MRI may have a role in differentiating meningiomas with atypical features on conventional imaging from malignant intra-axial tumours[65] and also in the prospective characterization of meningiomas. Yang *et al*. found mean

values of both rCBV (DSCE-MRI)) and K^{trans} to be lower in typical than atypical meningiomas[66].

Measurements of rCBV (DSCE-MRI) can also provide supplementary information to differentiate between malignant lymphoma and glioma because the absence of tumour neovascularization in malignant lymphoma leads to low rCBV in contrast to those of malignant gliomas[61]. Cha *et al*. in their series of 19 consecutive patients[67] with primary cerebral lymphoma found the maximum rCBV (DSCE-MRI) to be lower than that found in 51 patients with glioblastoma multiforme (GBM). These findings have been confirmed by subsequent studies[68]. Cha *et al*.[67] also identified DSCE-MRI as a useful diagnostic tool in differentiating tumefactive demyelinating lesions (TDL) from intracranial neoplasms. Early studies with ASL have also shown that the significantly higher tumour blood flow in GBMs compared with cerebral lymphomas allows effective differentiation with a threshold value of 1.2 for CBF, providing a sensitivity of 97%, specificity of 80%, positive predictive value (PPV) of 94%, and negative predictive value (NPV) of 89%[69]. This group also showed ASL to provide accuracy, sensitivity, and specificity for discrimination of neoplastic from non-neoplastic diseases of 90%, 97%, and 67%, respectively. Perfusion MRI has also been suggested as an effective clinical strategy for the differentiation of patients with primitive neuroectodermal tumours (PNET) from those with low-grade gliomas. Law *et al*.[70] found patients with low grade gliomas had significantly lower rCBV (DSCE-MRI, $p < 0.0005$) and K^{trans} ($p < 0.05$) than a comparative group of patients with PNET. However, comparison with a group of high grade gliomas showed no statistical significance in the rCBV and K^{trans}.

Glioma versus solitary metastasis

Perfusion MRI may assist in differentiating between primary gliomas and solitary cerebral metastasis. Rollin *et al*., in a study of diffusion and perfusion (DSCE-MRI) imaging, found mean rCBV values were higher for high-grade gliomas than for metastases, whilst the mean ADC values were higher for metastases[71]. Better discrimination can be obtained on the basis of the difference in peritumoral rCBV measurements[67,72,73]. In metastatic tumours, peritumoral oedema represents pure vasogenic oedema caused by increased interstitial water due to microvascular extravasation of plasma fluid and proteins through the inter-endothelial space[74,75]. In high grade gliomas the peritumoral region represents a variable combination of vasogenic oedema and tumour cells infiltrating along the perivascular space[75]. Similar findings have also been reported with ASL where CBF was significantly higher in peritumoral non-enhancing T2-hyperintense regions of glioblastomas compared with metastases; a threshold value of 0.5 for CBF provided sensitivity, specificity, PPV, and NPV of 100%, 71%, 94%, and 100%.

Glial cell tumours

In gliomas tumour capillary blood volumes measured by DSCE-MRI have been shown to correlate with and predict tumour grade[80–93] (Fig. 4). More importantly rCBV maps identify areas of malignant transformation or tumour dedifferentiation allowing more accurate targeting of stereotactic biopsies and therefore more accurate estimation of tumour grade[76,77]. An independent relationship between tumour grade and measurements of K^{trans} (both DSCE and DRCE-MRI) has also been demonstrated[78,79] although the correlation was less strong than that between grade and CBV (Fig. 5). Measurement of tumour blood flow using ASL also correlates with microvascular density in glioma and distinguishes between high- and low-grade tumours[80–82]. The relationship with grade is strengthened if measurements of tumour blood flow are compared to age-dependent mean brain perfusion[80]. Histological comparisons show close relationships between rCBV values (from both DSCE and DRCE-MRI) within tumours and histological features indicative of tumour aggression including mitotic activity and vascularity[83–86]. Comparison of imaging biomarkers with histological assessment of microvascular density (MVD) have also shown that MVD correlates with steepest slope of T1 first pass[35] and with CBV when histological measures are corrected for thickness effects[87].

Direct comparison between rCBV mapping and other indicators of malignancy such as fluorodeoxylucose PET shows close agreement between local rCBV values and glucose uptake and significant correlation between maximal glucose uptake and rCBV[88]. Comparison of CBV and methionine labelled PET also shows a close correlation between the techniques[89]. This is important since methionine PET commonly demonstrates tumour extension beyond the boundaries shown by conventional MRI and is currently being explored as a basis for radiotherapy planning[90,91]. Similar comparisons with thallium-201 SPECT show greater sensitivity to glioma grade[92] and higher sensitivity for demonstrating early tumour recurrence after therapy.
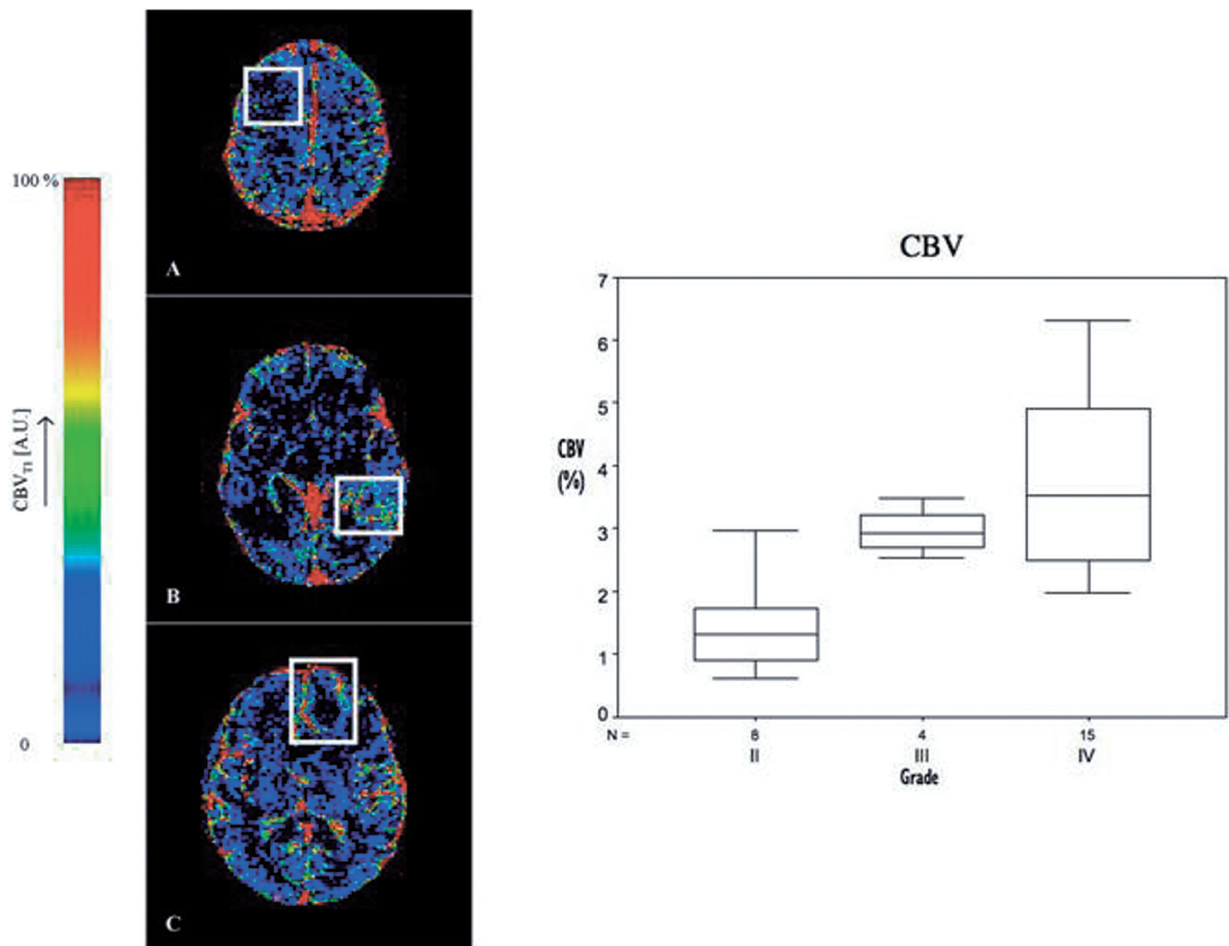
Figure 4   **CBV maps for (A) grade II diffuse fibrillary astrocytoma, (B) grade III anaplastic astrocytoma and (C) grade IV glioblastoma multiforme, from Patankar 2005[78]. Boxplot demonstrating increasing CBV with increasing tumour grade; from Mills *et al.*[99].**
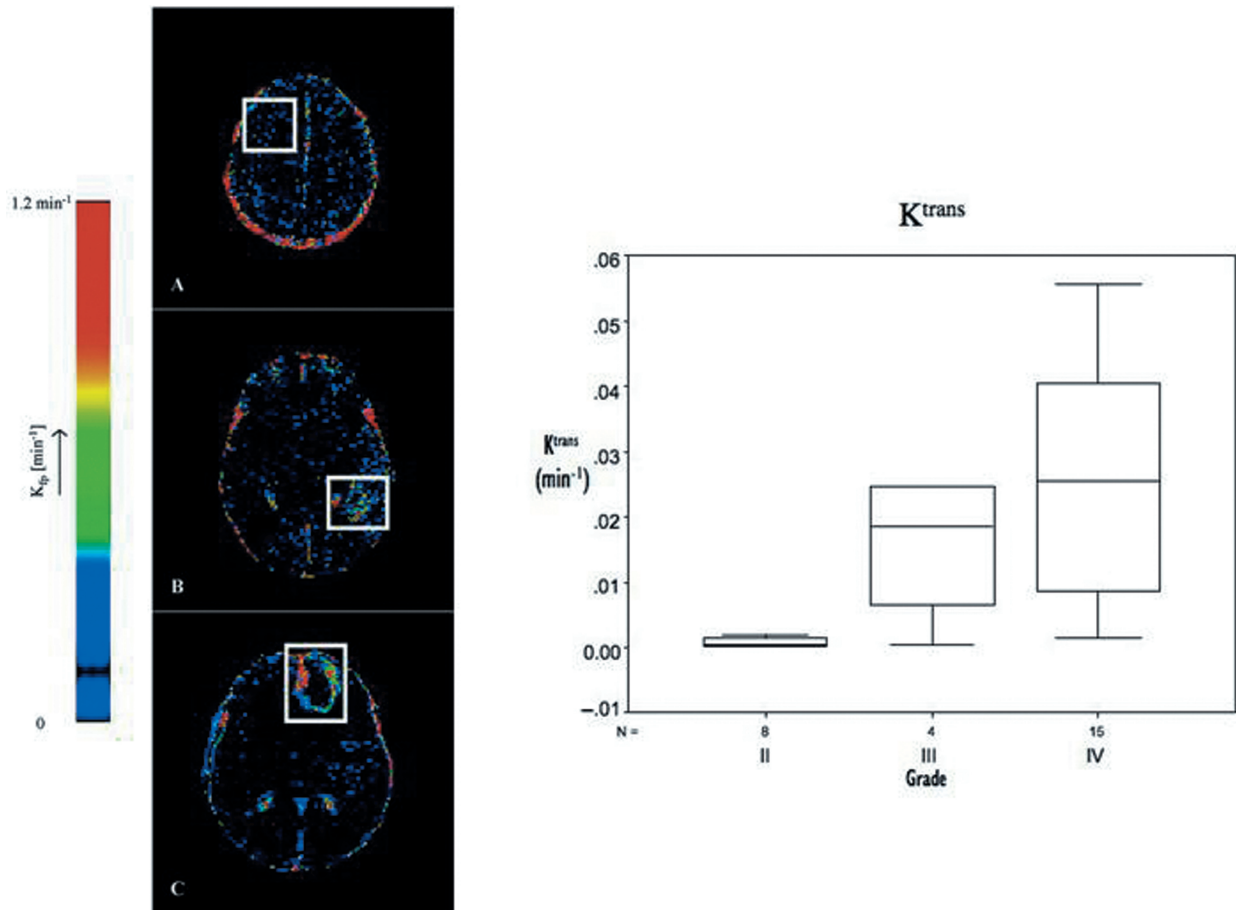
Figure 5 K^{trans} **maps for (A) grade II diffuse fibrillary astrocytoma, (B) grade III anaplastic astrocytoma and (C) grade IV glioblastoma multiforme, from Patankar *et al.*[78]. Boxplot demonstrating increasing K^{trans} with increasing tumour grade; from Mills *et al.*[99].**

There is also evidence of a significant relationship between imaging biomarkers and prognosis in patients with glioma. Early studies using non-pharmacokinetic analyses of enhancement data showed that delayed contrast uptake within glioma was associated with improved survival[93] and early pharmacokinetic studies using a simple two compartment model also showed that data from DCE-MRI prior to radiotherapy, together with changes occurring as a result of radiotherapy could identify patients who went on to show a decrease in tumour volume[76,94]. Subsequently, several groups have demonstrated a clear relationship between pre-operative CBV values within glioma, therapeutic response and survival[95–98]. In 2006, Mills *et al.* showed that this relationship mirrors the ability of CBV (DCRE-MRI) to predict tumour grade but that measurements of tumour K^{trans} predict disease-free and overall survival independently of both grade and CBV[99]. Recent studies using ASL have demonstrated that measurements of tumour blood flow can predict grade and 6-month response to surgical

treatment although it is unclear whether this is simply a correlation with the relationship between grade and survival[81].

Oligodendrogliomas

Oligodendroglial tumours represent more than 30% of glial tumours in adults and are characterized by a longer survival, better treatment response, and characteristic genetic alterations[100]. A significant proportion of oligodendrogliomas are characterized by a combined loss of chromosomes 1p and 19q, which is strongly associated with chemosensitivity in both primary and recurrent tumours and, in addition, correlates closely with loss of clear tumour margin on conventional imaging[101,102]. Unlike non-oligodendroglial gliomas, tumour contrast enhancement and normalized cerebral blood volume do not vary significantly between low- and high-grade oligodendrogliomas[103,104]. However, rCBV (DSCE-MRI) values are generally higher in oligodendroglioma than
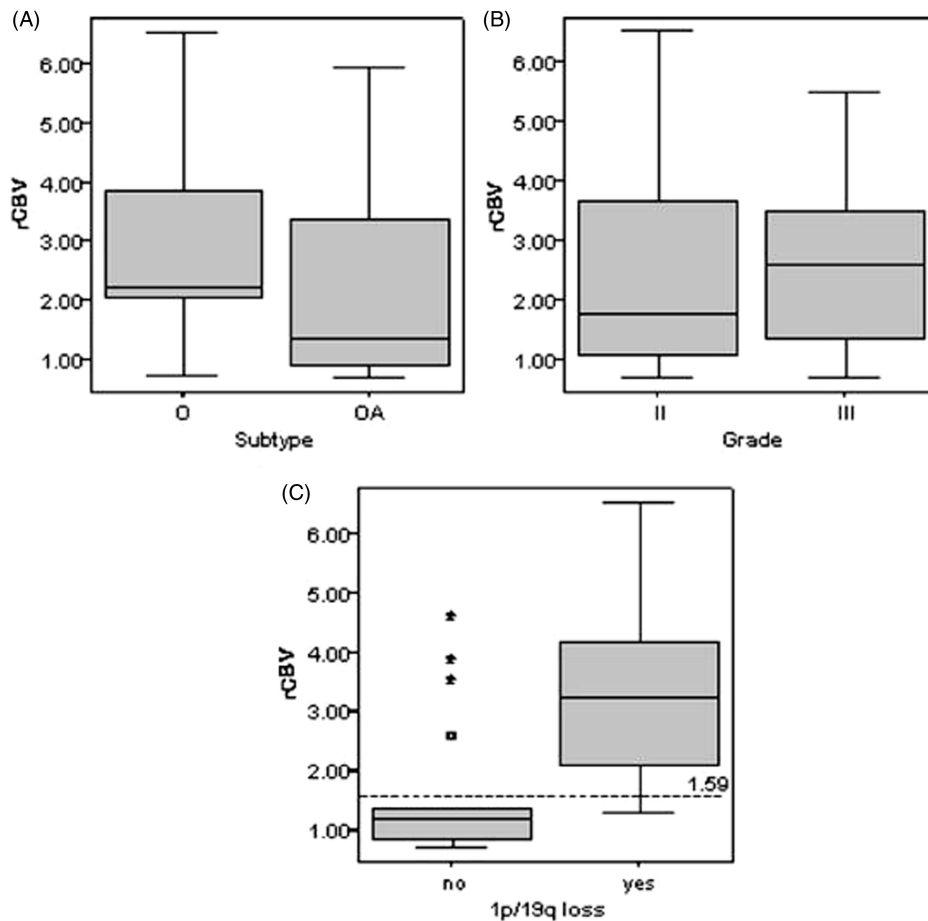
Figure 6 Box plots of rCBV against (A) histopathology subtype (*p* = 0.279*), (B) histopathology grade (*p* = 0.442*), and (C) genotype (*p* = 0.001*) in oligodendroglial tumours; from Jenkinson *et al.*[105] with permission.

in other benign brain tumours[95,104] and rCBV is particularly elevated in oligodendroglial tumours with 1p/19q loss, although it does not predict chemosensitivity[105,106] (Fig. 6). The prognostic significance of rCBV may differ in oligodendroglial tumours with or without the -1p/-19q genotype[105].

Imaging biomarkers and molecular/ genetic features

Genetic and molecular biomarkers also allow the identification of subtypes of glioblastoma. 'Primary glioblastoma' arising *de novo* in older patients and often overexpressing epidermal growth factor receptor (EGFR) is associated with increased antigenic activity. The 'secondary glioblastomas' progress from low-grade tumours in younger patients and commonly demonstrate TP53 mutations. These molecular subtypes have been associated with prognosis within the grade IV histological group suggesting that molecular markers offer realistic promise for the identification of glioma subtypes

over and above the information provided by histological grading. In glioblastoma, measurements of K^{trans} have been shown to predict prognosis in grade IV tumours independent of grade or other biomarkers[99]. In addition, EGFR amplification in glioblastoma correlates closely with the loss of border definition on T2-weighted images and an increase in the volume of brain showing T2 signal abnormality compared to the volume showing enhancement[107].

Therapeutic monitoring

Standard therapy

Treatment of high grade glioma consists of conformal radiotherapy (60 Gy in 30 fractions) with concurrent and adjuvant temozolomide[108,109]. Several workers have documented radiation induced changes in normal brain and tumours, including gliomas and meningiomas[110,111]. These studies have shown short-term increases and medium to long-term decreases in K^{trans}

in response to radiation therapy in both normal brain and tumour. More importantly some studies have shown that DRCE-MRI can differentiate between patients who show subsequent local tumour control and those who do not[94]. Other workers have also suggested that dynamic contrast-enhanced techniques may be useful in differentiating between tumour recurrence, characterized by high CBV and K^{trans}, and radiation necrosis characterized by low values[19,21,35,112–116]. However, radiation necrosis represents a heterogeneous process with features resembling inflammation. Immature vessels may grow into previously necrotic areas[117], and viable tumour cells may still be found in the areas with decreased blood volume. Therefore, when this technique is used to monitor irradiated areas, the risk of overlooking active tumour sites cannot be excluded[61].

There has been considerable interest in the use of imaging biomarkers to predict radiotherapy responsiveness and MRI diffusion imaging techniques appear to be particularly promising in this regard[118]. Cao *et al.* demonstrated that the percentage of the tumour showing high perfusion (DSCE-MRI) before radiotherapy and the fluid-attenuated inversion recovery imaging measures of tumour volume were predictors for survival ($p = 0.01$). Changes in tumour CBV during the early treatment course also predicted survival. Better survival was predicted by a decrease in the fractional low-CBV tumour volume at week 1 of radiotherapy[98]. Interestingly, there is no documented value of perfusion imaging for detecting or predicting response to temozolomide[119] although methionine PET imaging has been shown to predict clinical stability and a reduction in methionine uptake during temozolomide treatment predicts a favourable clinical outcome[120].

Antiangiogenic agents

Imaging biomarkers from dynamic contrast-enhanced imaging have been widely used in clinical trials of anti-angiogenic and vascular targeting agents outside the head[6]. These markers show early evidence of biological activity and commonly show a significant relationship with progression-free and overall survival and have now become a standard part of most trials of novel anti-angiogenic therapies. Anti-angiogenic therapies have only recently been trialled in patients with glioma although there is significant evidence that they are effective in this condition. Trials of carboplatin and thalidomide, which has anti-angiogenic activity, have shown significant decreases in rCBV (DSCE-MRI) and an association between larger decreases and response[121]. A Phase II trial of bevacizumab and irinotecan in recurrent malignant glioma showed a radiographic response rate of 63% with 1 complete remission and 19 partial responses from a total of 32 patients although advanced imaging by markers was not measured. A similar small-scale study examining the effect of AZD2171, an oral tyrosine kinase inhibitor of vascular endothelial growth factor (VEGF)

receptors, demonstrated clinical responses and significant prognostic changes in CBV (DRCE-MRI) and K^{trans}. This study also reported normalization of mean vessel diameter which has previously been demonstrated only from histological studies of anti-angiogenic therapy[24].

Future developments

Novel biomarkers

A number of other potential biomarkers of microvascular structure and function have been identified which are likely to become of increasing importance. These include both (a) novel data analysis based on current imaging techniques and (b) novel data acquisition.

Jackson *et al.*[7,122,123] described the failure of the contrast concentration time course curve to return to the expected level following the first passage of the contrast bolus — named relative recirculation (rR). Unlike rCBV and rCBF measurements, the rR parameter is affected only by areas of local ischaemia, decreased perfusion pressure or vascular tortuosity. Changes are, therefore, typically seen at the boundary between well-vascularized peripheral growing tissue and central tumour necrosis in high grade gliomas. Other workers have used a similar measurement of the percentage recovery of the contrast concentration curve from the peak value observed during passage of the bolus. This value in peritumoural white matter has been shown to differentiate between glioma and metastasis[37] and between glioma grade[38]. Heterogeneity analyses may also yield further biomarkers of tumour biology[124].

Several workers have examined the responses of the tumour microvasculature to physiological stimuli, particularly inhalation of carbon dioxide and oxygen using T2*-weighted MRI techniques. In a study of 10 patients with meningioma, the changes were variable with an increase in six and a decrease in four, although there was a clear correlation with the rate of contrast uptake[125]. In gliomas, large signal changes in the region of 25% were seen at the perimeter of tumours extending, at a lower magnitude, into the peritumoral areas, which did not show enhancement, but gave an abnormal signal on T2-weighted images[126]. Clinical application of such techniques is not yet proven, but these preliminary findings suggest that a combination of microvascular imaging biomarkers and physiological stimuli may be of value in assessing vascular reactivity and possibly regional hypoxia within the tumour.

Conclusions

The use of parametric imaging and imaging-based biomarkers in neuro-oncology is becoming increasingly routine and well established. Major technical challenges remain and must be overcome to ensure biomarker

validation. Nonetheless, in the next decade we are likely to see increasing standardization of image acquisition and analysis techniques in order to allow these clearly important imaging techniques to pass into routine research and clinical practice.

Acknowledgements

References

[1] Jackson A, Buckley DL, Parker GJM, editors. Dynamic contrast-enhanced magnetic resonance imaging in oncology. Berlin: Springer-Verlag; 2005, p. 1–311.

[2] Biomarkers Definitions Working Group. Biomarkers and surrogate endpoints: preferred definitions and conceptual framework. Clin Pharmacol Ther 2001; 69: 89–95.

[3] Lund EL, Spang-Thomsen M, Skovgaard-Poulsen H, Kristjansen PE. Tumor angiogenesis — a new therapeutic target in gliomas. Acta Neurol Scand 1998; 97: 52–62.

[4] Zhu XP, Li KL, Kamaly-Asl ID, Waterton J, Jackson A. Quantification of endothelial permeability, leakage space and blood volume in brain tumors using combined T1 and T2* contrast-enhanced dynamic MR imaging. J Magn Reson Imaging 2000; 11: 575–85.

[5] Jayson GC, Zweit J, Jackson A *et al.* Molecular imaging and biological evaluation of HuMV833 anti-VEGF antibody: implications for trial design of antiangiogenic antibodies. J Natl Cancer Inst 2002; 94: 1484–93.

[6] O'Connor JP, Jackson A, Parker GJ, Jayson GC. DCE-MRI biomarkers in the clinical evaluation of antiangiogenic and vascular disrupting agents. Br J Cancer 2007; 96: 189–95.

[7] Kassner A, Annesley D, Zhu XP *et al.* Abnormalities of the contrast re-circulation phase in cerebral tumors demonstrated using dynamic susceptibility contrast-enhanced imaging: a possible marker of vascular tortuosity. J Magn Reson Imaging 2000; 11: 103–13.

[8] Uematsu H, Maeda M, Sadato N *et al.* Vascular permeability: quantitative measurement with double-echo dynamic MR imaging — theory and clinical application. Radiology 2000; 214: 912–7.

[9] Knopp MV, Weiss E, Sinn HP, Gaa J, Laub G, Wielopolski P. Pathophysiologic basis of contrast enhancement in breast tumors. J Magn Reson Imaging 1999; 10: 260–6.

[10] Edelman RR, Siewert B, Adamis M *et al.* Signal targeting with alternating radiofrequency (STAR) sequences: application to MR angiography. Magn Reson Med 1994; 31: 233–8.

[11] Kwong KK, Chesler DA, Weisskoff RM *et al.* MR perfusion studies with T1-weighted echo planar imaging. Magn Reson Med 1995; 34: 878–87.

[12] Kim SG. Quantification of relative cerebral blood flow change by flow-sensitive alternating inversion recovery (FAIR) technique: application to functional mapping. Magn Reson Med 1995; 34: 293–301.

[13] Golay X, Hendrikse J, Lim TC. Perfusion imaging using arterial spin labeling. Top Magn Reson Imaging 2004; 15: 10–27.

[14] Rosen BR, Belliveau JW, Buchbinder BR *et al.* Contrast agents and cerebral hemodynamics. Magn Reson Med 1991; 19: 285–92.

[15] Calamante F, Thomas DL, Pell GS, Wiersma J, Turner R. Measuring cerebral blood flow using magnetic resonance imaging techniques. J Cereb Blood Flow Metab 1999; 19: 701–35.

[16] Jackson A. Analysis of dynamic contrast enhanced MRI. Br J Radiol 2004; 77: S154–66.

[17] Barbier EL, Lamalle L, Decorps M. Methodology of brain perfusion imaging. J Magn Reson Imaging 2001; 13: 496–520.

[18] Sorensen A, Reimer P. Cerebral MR perfusion imaging: principles and current applications. Vol. 152. Stuttgart: Thieme; 2000.

[19] Boxerman JL, Hamberg L, Rosen B, Weisskoff RM. MR contrast due to intravascular magnetic susceptibility perturbations. Magn Reson Med 1995; 34: 555–66.

[20] Ostergaard L, Johannsen P, Host Poulsen P *et al.* Cerebral blood flow measurements by magnetic resonance imaging bolus tracking: comparison with [^{15}O]H$_2$O positron emission tomography in humans. J Cereb Blood Flow Metab 1998; 18: 935–40.

[21] Rosen BR, Belliveau JW, Aronen HJ *et al.* Susceptibility contrast imaging of cerebral blood volume: human experience. Magn Reson Med 1991; 22: 293–9 (discussion 300–3).

[22] Calamante F, Gadian DG, Connelly A. Delay and dispersion effects in dynamic susceptibility contrast MRI: simulations using singular value decomposition. Magn Reson Med 2000; 44: 466–73.

[23] Weisskoff RM, Zuo CS, Boxerman JL, Rosen BR. Microscopic susceptibility variation and transverse relaxation: theory and experiment. Magn Reson Med 1994; 31: 601–10.

[24] Batchelor TT, Sorensen AG, di Tomaso E *et al.* AZD2171, a pan-VEGF receptor tyrosine kinase inhibitor, normalizes tumor vasculature and alleviates edema in glioblastoma patients. Cancer Cell 2007; 11: 83–95.

[25] Donahue KM, Krouwer HG, Rand SD *et al.* Utility of simultaneously acquired gradient-echo and spin-echo cerebral blood volume and morphology maps in brain tumor patients. Magn Reson Med 2000; 43: 845–53.

[26] Jain RK. Normalization of tumor vasculature: an emerging concept in antiangiogenic therapy. Science 2005; 307: 58–62.

[27] Buckley DL, Parker GJM. Measuring contrast agent concentration in T1-weighted dynamic contrast-enhanced MRI. In: Jackson A, Buckley DL, Parker GJM, editors. Dynamic contrast-enhanced magnetic resonance imaging in oncology. Berlin: Springer-Verlag; 2005, p. 69–79.

[28] Parker GJ, Roberts C, Macdonald A *et al.* Experimentally-derived functional form for a population-averaged high-temporal-resolution arterial input function for dynamic contrast-enhanced MRI. Magn Reson Med 2006; 56: 993–1000.

[29] Li KL, Zhu XP, Jackson A. Parametric mapping of scaled fitting error in dynamic susceptibility contrast enhanced MR perfusion imaging. Br J Radiol 2000; 73: 470–81.

[30] Li KL, Zhu XP, Waterton J, Jackson A. Improved 3D quantitative mapping of blood volume and endothelial permeability in brain tumors. J Magn Reson Imaging 2000; 12: 347–57.

[31] Parker GJM, Buckley DL. Tracer kinetic modelling for T1-weighted DCE-MRI. In: Jackson A, Buckley DL, Parker GJM, editors. Dynamic contrast-enhanced magnetic resonance imaging in oncology. Berlin: Springer-Verlag; 2005, p. 81–92.

[32] Stack JP, Redmond O, Codd M, Dervan P, Ennis J. Breast disease: tissue characterization with Gd-DTPA enhancement profiles. Radiology 1990; 174: 491–4.

[33] Flickinger FW, Allison J, Sherry R *et al.* Differentiation of benign from malignant breast masses by time-intensity evaluation of contrast enhanced MRI. Magn Reson Imaging 1993; 11: 617–20.

[34] Roberts C, Issa B, Stone A, Jackson A, Waterton J, Parker G. Comparative study into the robustness of compartmental modeling and model-free analysis in DCE-MRI studies. J Magn Reson Imaging 2006; 23: 554–63.

[35] Maeda M, Itoh S, Kimura H *et al.* Tumor vascularity in the brain: evaluation with dynamic susceptibility-contrast MR imaging. Radiology 1993; 189: 233–8.

[36] Provenzale JM, York G, Moya MG *et al.* Correlation of relative permeability and relative cerebral blood volume in high-grade cerebral neoplasms. AJR Am J Roentgenol 2006; 187: 1036–42.

[37] Cha S, Lupo JM, Chen MH et al. Differentiation of glioblastoma multiforme and single brain metastasis by peak height and percentage of signal intensity recovery derived from dynamic susceptibility-weighted contrast-enhanced perfusion MR imaging. AJNR Am J Neuroradiol 2007; 28: 1078–84.

[38] Lupo JM, Cha S, Chang SM, Nelson SJ. Dynamic susceptibility-weighted perfusion imaging of high-grade gliomas: characterization of spatial heterogeneity. AJNR Am J Neuroradiol 2005; 26: 1446–54.

[39] Tofts PS. Modeling tracer kinetics in dynamic Gd-DTPA MR imaging. J Magn Reson Imaging 1997; 7: 91–101.

[40] Tofts PS, Brix G, Buckley DL et al. Estimating kinetic parameters from dynamic contrast-enhanced T1-weighted MRI of a diffusable tracer: standardized quantities and symbols. J Magn Reson Imaging 1999; 10: 223–32.

[41] Tofts PS, Kermode AG. Measurement of the blood-brain barrier permeability and leakage space using dynamic MR imaging. Magn Reson Med 1991; 17: 357–67.

[42] Padhani AR, Husband JE. Dynamic contrast-enhanced MRI studies in oncology with an emphasis on quantification, validation and human studies. Clin Radiol 2001; 56: 607–20.

[43] Leach MO, Brindle KM, Evelhoch JL et al. Assessment of anti-angiogenic and antivascular therapeutics using MRI: recommendations for appropriate methodology for clinical trials. Br J Radiol 2003; 76: S87–91.

[44] Leach MO, Brindle KM, Evelhoch JL et al. The assessment of antiangiogenic and antivascular therapies in early-stage clinical trials using magnetic resonance imaging: issues and recommendations. Br J Cancer 2005; 92: 1599–610.

[45] Haroon HA, Buckley DL, Patankar TA et al. A comparison of K^{trans} measurements obtained with conventional and first pass pharmacokinetic models in human gliomas. J Magn Reson Imaging 2004; 19: 527–36.

[46] St Lawrence KS, Lee TY. An adiabatic approximation to the tissue homogeneity model for water exchange in the brain: I. Theoretical derivation. J Cereb Blood Flow Metab 1998; 18: 1365–77.

[47] Calamante F, Gadian DG, Connelly A. Quantification of perfusion using bolus tracking magnetic resonance imaging in stroke: assumptions, limitations, and potential implications for clinical use. Stroke 2002; 33: 1146–51.

[48] Ostergaard L, Hochberg FH, Rabinov JD et al. Early changes measured by magnetic resonance imaging in cerebral blood flow, blood volume, and blood–brain barrier permeability following dexamethasone treatment in patients with brain tumors. J Neurosurg 1999; 90: 300–5.

[49] Thacker NA, Scott ML, Jackson A. Can dynamic susceptibility contrast magnetic resonance imaging perfusion data be analyzed using a model based on directional flow? J Magn Reson Imaging 2003; 17: 241–55.

[50] St Lawrence KS, Lee TY. An adiabatic approximation to the tissue homogeneity model for water exchange in the brain: II. Experimental validation. J Cereb Blood Flow Metab 1998; 18: 1378–85.

[51] Jayson GC, Parker GJ, Mullamitha S et al. Blockade of platelet-derived growth factor receptor-beta by CDP860, a humanized, PEGylated di-Fab′, leads to fluid accumulation and is associated with increased tumor vascularized volume. J Clin Oncol 2005; 23: 973–81.

[52] Buckley DL. Uncertainty in the analysis of tracer kinetics using dynamic contrast-enhanced T1-weighted MRI. Magn Reson Med 2002; 47: 601–6.

[53] Haroon HA, Patankar TF, Zhu XP et al. Comparison of cerebral blood volume maps generated from T2* and T1 weighted MRI data in intra-axial cerebral tumours. Br J Radiol 2007; 80: 161–8.

[54] Erdogan C, Hakyemez B, Yildirim N, Parlak M. Brain abscess and cystic brain tumor: discrimination with dynamic susceptibility contrast perfusion-weighted MRI. J Comput Assist Tomogr 2005; 29: 663–7.

[55] Holmes TM, Petrella JR, Provenzale JM. Distinction between cerebral abscesses and high-grade neoplasms by dynamic susceptibility contrast perfusion MRI. AJR Am J Roentgenol 2004; 183: 1247–52.

[56] Foo SS, Abbott D, Lawrentschuk N, Scott A. Functional imaging of intratumoral hypoxia. Mol Imaging Biol 2004; 6: 291–305.

[57] Bink A, Gaa J, Franz K et al. Importance of diffusion-weighted imaging in the diagnosis of cystic brain tumors and intracerebral abscesses. Zentralbl Neurochir 2005; 66: 119–25.

[58] Mascalchi M, Filippi M, Floris R, Fonda C, Gasparrotti R, Villari N. Diffusion-weighted MR of the brain: methodology and clinical application. Radiol Med (Torino) 2005; 109: 155–97.

[59] Fujii K, Fujita N, Hirabuki N, Hashimoto T, Miura T, Kozuka T. Neuromas and meningiomas: evaluation of early enhancement with dynamic MR imaging. AJNR Am J Neuroradiol 1992; 13: 1215–20.

[60] Nagele T, Petersen D, Klose U et al. Dynamic contrast enhancement of intracranial tumors with snapshot-FLASH MR imaging. AJNR Am J Neuroradiol 1993; 14: 89–98.

[61] Sugahara T, Korogi Y, Shigematsu Y et al. Value of dynamic susceptibility contrast magnetic resonance imaging in the evaluation of intracranial tumors. Top Magn Reson Imaging 1999; 10: 114–24.

[62] Maeda M, Itoh S, Kimura H et al. Vascularity of meningiomas and neuromas: assessment with dynamic susceptibility-contrast MR imaging. AJR Am J Roentgenol 1994; 163: 181–6.

[63] Miyati T, Banno T, Mase M et al. Dual dynamic contrast-enhanced MR imaging. J Magn Reson Imaging 1997; 7: 230–5.

[64] Long DM. Vascular ultrastructure in human meningiomas and schwannomas. J Neurosurg 1973; 38: 409–19.

[65] Hakyemez B, Yildirim N, Erdogan C, Kocaeli H, Korfali E, Parlak M. Meningiomas with conventional MRI findings resembling intraaxial tumors: can perfusion-weighted MRI be helpful in differentiation? Neuroradiology 2006; 48: 695–702.

[66] Yang S, Law M, Zagzag D et al. Dynamic contrast-enhanced perfusion MR imaging measurements of endothelial permeability: differentiation between atypical and typical meningiomas. AJNR Am J Neuroradiol 2003; 24: 1554–9.

[67] Cha S, Knopp EA, Johnson G, Wetzel SG, Litt AW, Zagzag D. Intracranial mass lesions: dynamic contrast-enhanced susceptibility-weighted echo-planar perfusion MR imaging. Radiology 2002; 223: 11–29.

[68] Calli C, Kitis O, Yunten N, Yurtseven T, Islekel S, Akalin T. Perfusion and diffusion MR imaging in enhancing malignant cerebral tumors. Eur J Radiol 2006; 58: 394–403.

[69] Weber MA, Zoubaa S, Schlieter M et al. Diagnostic performance of spectroscopic and perfusion MRI for distinction of brain tumors. Neurology 2006; 66: 1899–906.

[70] Law M, Kazmi K, Wetzel S et al. Dynamic susceptibility contrast-enhanced perfusion and conventional MR imaging findings for adult patients with cerebral primitive neuroectodermal tumors. AJNR Am J Neuroradiol 2004; 25: 997–1005.

[71] Rollin N, Guyotat J, Streichenberger N, Honnorat J, Tran Minh V-A, Cotton F. Clinical relevance of diffusion and perfusion magnetic resonance imaging in assessing intra-axial brain tumors. Neuroradiology 2006; 48: 150–9.

[72] Cha S, Law M, Johnson G et al. Peritumoral region: differentiation between primary high-grade neoplasm and solitary metastasis using dynamic contrast-enhanced T2*-weighted echo-planar perfusion MR imaging. In: Proceedings of the 38th Annual Meeting of the American Society of Neuroradiology, 2000, Atlanta, GA.

[73] Chiang IC, Kuo YT, Lu CY et al. Distinction between high-grade gliomas and solitary metastases using peritumoral 3-T magnetic resonance spectroscopy, diffusion, and perfusion imagings. Neuroradiology 2004; 46: 619–27.

[74] Strugar J, Rothbart D, Harrington W, Criscuolo GR. Vascular permeability factor in brain metastases: correlation with vasogenic brain edema and tumor angiogenesis. J Neurosurg 1994; 81: 560–6.

[75] Strugar JG, Criscuolo GR, Rothbart D, Harrington W. Vascular endothelial growth/permeability factor expression in human glioma specimens: correlation with vasogenic brain edema and tumor-associated cysts. J Neurosurg 1995; 83: 682–9.

[76] Knopp EA, Cha S, Johnson G et al. Glial neoplasms: dynamic contrast-enhanced T2*-weighted MR imaging. Radiology 1999; 211: 791–8.

[77] Di Costanzo A, Scarabino T, Trojsi F et al. Multiparametric 3T MR approach to the assessment of cerebral gliomas: tumor extent and malignancy. Neuroradiology 2006; 48: 622–31.

[78] Patankar TF, Haroon HA, Mills SJ et al. Is volume transfer coefficient (K(trans)) related to histologic grade in human gliomas? AJNR Am J Neuroradiol 2005; 26: 2455–65.

[79] Law M, Yang S, Babb JS et al. Comparison of cerebral blood volume and vascular permeability from dynamic susceptibility contrast-enhanced perfusion MR imaging with glioma grade. AJNR Am J Neuroradiol 2004; 25: 746–55.

[80] Warmuth C, Gunther M, Zimmer C. Quantification of blood flow in brain tumors: comparison of arterial spin labeling and dynamic susceptibility-weighted contrast-enhanced MR imaging. Radiology 2003; 228: 523–32.

[81] Brown GG, Clark C, Liu TT. Measurement of cerebral perfusion with arterial spin labeling: Part 2. Applications. J Int Neuropsychol Soc 2007; 13: 526–38.

[82] Kimura H, Takeuchi H, Koshimoto Y et al. Perfusion imaging of meningioma by using continuous arterial spin-labeling: comparison with dynamic susceptibility-weighted contrast-enhanced MR images and histopathologic features. AJNR Am J Neuroradiol 2006; 27: 85–93.

[83] Aronen HJ, Glass J, Pardo FS et al. Echo-planar MR cerebral blood volume mapping of gliomas. Clinical utility. Acta Radiol 1995; 36: 520–8.

[84] Sugahara T, Korogi Y, Kochi M et al. Correlation of MR imaging-determined cerebral blood volume maps with histologic and angiographic determination of vascularity of gliomas. AJR Am J Roentgenol 1998; 171: 1479–86.

[85] Roberts HC, Roberts TP, Brasch RC, Dillon WP. Quantitative measurement of microvascular permeability in human brain tumors achieved using dynamic contrast-enhanced MR imaging: correlation with histologic grade. AJNR Am J Neuroradiol 2000; 21: 891–9.

[86] Roberts HC, Roberts TP, Bollen AW, Ley S, Brasch RC, Dillon WP. Correlation of microvascular permeability derived from dynamic contrast-enhanced MR imaging with histologic grade and tumor labeling index: a study in human brain tumors. Acad Radiol 2001; 8: 384–91.

[87] Pathak AP, Schmainda KM, Ward BD, Linderman JR, Rebro KJ, Greene AS. MR-derived cerebral blood volume maps: issues regarding histological validation and assessment of tumor angiogenesis. Magn Reson Med 2001; 46: 735–47.

[88] Aronen HJ, Pardo FS, Kennedy DN et al. High microvascular blood volume is associated with high glucose uptake and tumor angiogenesis in human gliomas. Clin Cancer Res 2000; 6: 2189–200.

[89] Sadeghi N, Salmon I, Tang BN et al. Correlation between dynamic susceptibility contrast perfusion MRI and methionine metabolism in brain gliomas: preliminary results. J Magn Reson Imaging 2006; 24: 989–94.

[90] Grosu AL, Piert M, Weber WA et al. Positron emission tomography for radiation treatment planning. Strahlenther Onkol 2005; 181: 483–99.

[91] Grosu AL, Weber WA, Franz M et al. Reirradiation of recurrent high-grade gliomas using amino acid PET (SPECT)/CT/MRI image fusion to determine gross tumor volume for stereotactic fractionated radiotherapy. Int J Radiat Oncol Biol Phys 2005; 63: 511–9.

[92] Lam WW, Chan KW, Wong WL, Poon WS, Metriweli C. Pre-operative grading of intracranial glioma. Acta Radiol 2001; 42: 548–54.

[93] Wong ET, Jackson EF, Hess KR et al. Correlation between dynamic MRI and outcome in patients with malignant gliomas. Neurology 1998; 50: 777–81.

[94] Hawighorst H, Knopp MV, Debus J et al. Pharmacokinetic MRI for assessment of malignant glioma response to stereotactic radiotherapy: initial results. J Magn Reson Imaging 1998; 8: 783–8.

[95] Lev MH, Ozsunar Y, Henson JW et al. Glial tumor grading and outcome prediction using dynamic spin-echo MR susceptibility mapping compared with conventional contrast-enhanced MR: confounding effect of elevated rCBV of oligodendrogliomas [corrected]. AJNR Am J Neuroradiol 2004; 25: 214–21.

[96] Law M, Oh S, Babb JS et al. Low-grade gliomas: dynamic susceptibility-weighted contrast-enhanced perfusion MR imaging – prediction of patient clinical response. Radiology 2006; 238: 658–67.

[97] Chaskis C, Stadnik T, Michotte A, Van Rompaey K, D'Haens J. Prognostic value of perfusion-weighted imaging in brain glioma: a prospective study. Acta Neurochir (Wien) 2006; 148: 277–85; discussion 285.

[98] Cao Y, Tsien CI, Nagesh V et al. Survival prediction in high-grade gliomas by MRI perfusion before and during early stage of RT [corrected]. Int J Radiat Oncol Biol Phys 2006; 64: 876–85.

[99] Mills SJ, Patankar TA, Haroon HA, Balériauxc D, Swindellb R, Jackson A. Do cerebral blood volume and contrast transfer coefficient predict prognosis in human glioma? AJNR Am J Neuroradiol 2006; 27: 853–8.

[100] Roux FX, Nataf F. Cerebral oligodendrogliomas in adults and children. Current data and perspectives. Neurochirurgie 2005; 51: 410–4.

[101] Cairncross JG, Ueki K, Zlatescu KC et al. Specific genetic predictors of chemotherapeutic response and survival in patients with anaplastic oligodendrogliomas. J Natl Cancer Inst 1998; 90: 1473–9.

[102] Ino Y, Betensky RA, Zlatescu MC et al. Molecular subtypes of anaplastic oligodendroglioma: implications for patient management at diagnosis. Clin Cancer Res 2001; 7: 839–45.

[103] Xu M, See SJ, Ng WH et al. Comparison of magnetic resonance spectroscopy and perfusion-weighted imaging in presurgical grading of oligodendroglial tumors. Neurosurgery 2005; 56: 919–26; discussion 919–26.

[104] White ML, Zhang Y, Kirby P, Ryken TC. Can tumor contrast enhancement be used as a criterion for differentiating tumor grades of oligodendrogliomas? AJNR Am J Neuroradiol 2005; 26: 784–90.

[105] Jenkinson MD, Smith TS, Joyce KA et al. Cerebral blood volume, genotype and chemosensitivity in oligodendroglial tumours. Neuroradiology 2006; 48: 703–13.

[106] Law M, Brodsky JE, Babb J et al. High cerebral blood volume in human gliomas predicts deletion of chromosome 1p: preliminary results of molecular studies in gliomas with elevated perfusion. J Magn Reson Imaging 2007; 25: 1113–9.

[107] Aghi M, Gaviani P, Henson JW, Batchelor TT, Louis DN, Barker FG. Magnetic resonance imaging characteristics predict epidermal growth factor receptor amplification status in glioblastoma. Clin Cancer Res 2005; 11: 8600–5.

[108] Bleehen NM, Stenning SP. A Medical Research Council trial of two radiotherapy doses in the treatment of grades 3 and 4 astrocytoma. The Medical Research Council Brain Tumour Working Party. Br J Cancer 1991; 64: 769–74.

[109] Laperriere N, Zuraw L, Cairncross G. Radiotherapy for newly diagnosed malignant glioma in adults: a systematic review. Radiother Oncol 2002; 64: 259–73.

[110] Wenz F, Rempp K, Hess T et al. Effect of radiation on blood volume in low-grade astrocytomas and normal brain tissue: quantification with dynamic susceptibility contrast MR imaging. AJR Am J Roentgenol 1996; 166: 187–93.

[111] Fuss M, Wenz F, Scholdei R et al. Radiation-induced regional cerebral blood volume (rCBV) changes in normal brain and low-

grade astrocytomas: quantification and time and dose-dependent occurrence. Int J Radiat Oncol Biol Phys 2000; 48: 53—8.

[112] Alavi JB, Alavi A, Chawluk A *et al.* Positron emission tomography in patients with glioma. A predictor of prognosis. Cancer 1988; 62: 1074—8.

[113] Frahm J, Haase A, Matthaei D. Rapid three-dimensional MR imaging using the FLASH technique. J Comput Assist Tomogr 1986; 10: 363—8.

[114] Reinhold HS, Endrich B. Tumour microcirculation as a target for hyperthermia. Int J Hyperthermia 1986; 2: 111—37.

[115] Song CW, Lokshina A, Rhee JG, Patten M, Levitt SH. Implication of blood flow in hyperthermic treatment of tumors. IEEE Trans Biomed Eng 1984; 31: 9—16.

[116] Rosen BR, Aronen HJ, Kwong KK, Belliveau JW, Hamberg LM, Fordham JA. Advances in clinical neuroimaging: functional MR imaging techniques. Radiographics 1993; 13: 889—96.

[117] Gobbel GT, Seilhan TM, Fike JR. Cerebrovascular response after interstitial irradiation. Radiat Res 1992; 130: 236—40.

[118] Herholz K, Coope D, Jackson A. Metabolic and molecular imaging in neuro-oncology. Lancet Neurol 2007; 6: 711—24.

[119] Leimgruber A, Ostermann S, Yeon EJ *et al.* Perfusion and diffusion MRI of glioblastoma progression in a four-year prospective temozolomide clinical trial. Int J Radiat Oncol Biol Phys 2006; 64: 869—75.

[120] Galldiks N, Kracht LW, Burghaus L *et al.* Use of ^{11}C-methionine PET to monitor the effects of temozolomide chemotherapy in malignant gliomas. Eur J Nucl Med Mol Imaging 2006; 33: 516—24.

[121] Cha S, Knopp EA, Johnson G *et al.* Dynamic contrast-enhanced T2-weighted MR imaging of recurrent malignant gliomas treated with thalidomide and carboplatin. AJNR Am J Neuroradiol 2000; 21: 881—90.

[122] Jackson A, Kassner A, Annesley-Williams D, Reid H, Zhu XP, Li KL. Abnormalities in the recirculation phase of contrast agent bolus passage in cerebral gliomas: comparison with relative blood volume and tumor grade. AJNR Am J Neuroradiol 2002; 23: 7—14.

[123] Jackson A, Kassner A, Zhu XP, Li KL. Reproducibility of T2* blood volume and vascular tortuosity maps in cerebral gliomas. J Magn Reson Imaging 2001; 14: 510—6.

[124] Jackson A, O'Connor JPB, Parker GJM, Jayson GC. Imaging tumor vascular heterogeneity and angiogenesis using dynamic contrast-enhanced magnetic resonance imaging. Clin Cancer Res 2007; 13: 3449—59.

[125] Rijpkema M, Schuuring J, Bernsen PL *et al.* BOLD MRI response to hypercapnic hyperoxia in patients with meningiomas: correlation with gadolinium-DTPA uptake rate. Magn Reson Imaging 2004; 22: 761—7.

[126] Rauscher A, Sedlacik J, Fitzek C *et al.* High resolution susceptibility weighted MR-imaging of brain tumors during the application of a gaseous agent. Rofo 2005; 177: 1065—9.